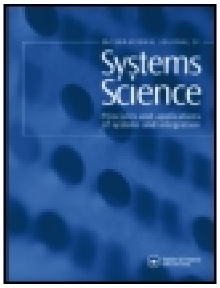

International Journal of Systems Science
Publication details, including instructions for authors and subscription information:
http://www.tandfonline.com/loi/tsys20

Sliding-mode and proportional-derivative-type motion control with radial basis function neural network based estimators for wheeled vehicles

Anugrah K. Pamosoaji [a] , Pham Thuong Cat [b] & Keum-Shik Hong [a c]

[a] School of Mechanical Engineering, Pusan National University, Busan, Korea

[b] Department of Automation Technology, Institute of Information Technology, Hanoi, Vietnam

[c] Department of Cogno-Mechatronics Engineering, Pusan National University, Busan, Korea
Version of record first published: 04 Mar 2013.

International Journal of Systems Science, 2013
http://dx.doi.org/10.1080/00207721.2013.772678

Sliding-mode and proportional-derivative-type motion control with radial basis function neural network based estimators for wheeled vehicles

Anugrah K. Pamosoaji[a], Pham Thuong Cat[b] and Keum-Shik Hong[a,c,*]

[a]*School of Mechanical Engineering, Pusan National University, Busan, Korea;* [b]*Department of Automation Technology, Institute of Information Technology, Hanoi, Vietnam;* [c]*Department of Cogno-Mechatronics Engineering, Pusan National University, Busan, Korea*

(*Received 3 July 2012; final version received 21 January 2013*)

An obstacle avoidance problem of rear-steered wheeled vehicles in consideration of the presence of uncertainties is addressed. Modelling errors and additional uncertainties are taken into consideration. Controller designs for driving and steering motors are designed. A proportional-derivative-type driving motor controller and a sliding-mode steering controller combined with radial basis function neural network (RBFNN) based estimators are proposed. The convergence properties of the RBFNN-based estimators are proven by the Stone–Weierstrass theorem. The stability of the proposed control law is proven using Lyapunov stability analysis. The obstacle avoidance strategy utilising the sliding surface adjustment to an existing navigation method is presented. It is concluded that the driving velocity and steering-angle performances of the proposed control system are satisfactory.

Keywords: obstacle avoidance; wheeled vehicle; estimation; sliding-mode control; proportional derivative control; radial basis function networks

1. Introduction

As robotics become increasingly sophisticated, obstacle avoidance emerges as an ever-more important aspect of motion control. In most motion-controller design cases, a vehicle, for the purposes of analytical simplification, is assumed to be free of modelling errors and additional uncertainties (Fraichard and Asama 2004). Under certain conditions, this approach is useful for determining the vehicle behaviour and for elucidating various significant properties in motion-control studies. However, in practical cases, theoretical and simplified behaviours regularly result in large errors (Widyotriatmo, Hong, and Hong 2009). In designing an obstacle-avoidance strategy therefore the distinction between theoretical and practical behaviours should be as small as possible.

Generally, obstacle-avoidance strategies are integrated into motion-control designs. Various motion-control solutions of this type have been reported: Examples include the potential field approach (Huang 2009), backstepping (Wu, Shi, and Gao 2010; Cheng, Su, and Tsai 2012) and sliding-mode control techniques (Chwa 2004; Shi, Xia, Liu, and Rees 2006; Park, Yoo, Park, and Choi 2009; Fallaha, Saad, Kanaan, and Al-Haddad 2011; Lin, Xia, Shi, and Wu 2011; Chang, Chang, Chen, and Tao 2012; Gan and Liang 2012; Khan, Bhatti, Iqbal, and Ahmed 2012; Lin, Chang, and Hsu 2012; Ngo and Hong 2012a,b; Wu, Su, and Shi 2012; Zhao and Zhou 2012). In Widyotriatmo, Hong, and Prayudhi (2010) and Widyotriatmo and Hong (2011, 2012), a novel navigation function for a nonholonomic rear-steered wheeled vehicle was proposed. In those works, however, they did not take uncertainty into consideration.

The presence of uncertainties, particularly for nonholonomic wheeled vehicles, has obliged researchers to explore compensator design. Solutions involving neural networks are powerful approaches: A combined backstepping and neural-network-based method was reported in Fierro and Lewis (1998). In Schilling, Carroll, and Al-Ajlouni (2001), a method for nonlinear systems estimation using a radial basis function neural network (RBFNN) was proposed. However, it yielded only bounded-input, bounded-output stable outputs. Ge and Zhang (2003) proposed control of a non-affine nonlinear system with zero dynamics by means of a multilayer neural network. Xu, Zhao, Yi, and Tan (2009) applied a combined RBFNN/sliding-mode control for trajectory-tracking missions of an omnidirectional wheeled mobile manipulator. Bugeja, Fabri, and Camilleri (2009) proposed an adaptive control that utilises two types of neural networks: Gaussian radial basis function and sigmoidal multilayer perceptron neural network . Kasac, Deur, Novakovic, Kolmanovsky, and Assadian (2011) applied a backpropagation-through-time like optimal control algorithm to a 10-d.o.f. vehicle for optimisation of a trajectory-tracking controller. Chen (2011) incorporated a type of wavelet neural network into a proportional–integral–derivative type learning algorithm to enhance trajectory-tracking performance.

*Corresponding author. Email: kshong@pusan.ac.kr

The capability of neural networks as estimators was introduced in Hornik (1989, 1991), wherein it was claimed that multilayer feed-forward networks can be used as universal estimators. This fact was verified by the Stone–Weierstrass theorem (Cotter 1990), which states that multilayer feed-forward networks with dense and separable functions are acceptable as estimators. In the case of mechanical systems, several studies have applied neural networks for estimation purposes: Tsai, Chan, and Li (2012) addressed the issue of the reduction of friction effects in an H_∞ control scheme for brushless DC motors. Cheng et al. (2012) combined a sliding-mode controller with a fuzzy-neural-network-based friction estimator. Recently, neural network based optimisation approaches have been heavily investigated (Deng, Li, and Irwin 2012; Yang, Zhu, Yuan, and Meng 2012; Zhang and Chu 2012; Zhang, Zhu, and Yang 2012). However, the selection of an efficient number of membership functions in fuzzy control emerges as a new problem.

As material-handling vehicles in recent years have been widely adopted for use in complex environments, the issue of safety has emerged. The twin requirements (high speed and safe motion) have been the main research issues in this area. However, the consideration of input has brought the concept of collision-free configuration into question. Furthermore, the existence of modelling errors and additional uncertainties makes this issue more complicated still. For the purposes of safety analysis, Fraichard and Asama (2004) introduced the concept of inevitable collision state (ICS) as an alternative method to collision-free states/configurations. Typical collision-free configurations are defined as those without any intersection between the vehicle's body and any obstacle. However, under the application of particular inputs, configurations that are considered to be collision-free become, according to the ICS, prohibited configurations. The reason is based on the possibility of colliding for the next n time sampling. Chakravarthy and Ghose (2012) investigated this concept further by introducing 'collision cone' for consideration in the design of collision-avoidance strategies, in which a number of theories regarding conditions of possible collisions were proposed. However, their method lacks any discussion on the effects of uncertainties.

In this paper, an obstacle-avoidance strategy for a type of a rear-steered wheeled vehicle operating under the conditions of modelling errors and uncertainties is presented. Since modelling errors and additional uncertainties can arise in voltage-to-torque conversions of the driving and steering motors, we designed a voltage-input control law rather than a torque control law. Control of the driving motor's voltage is achieved as the proportional-derivative (PD) type, and that of the steering angle is obtained in the sliding mode. To reduce the effect of modelling errors and additional uncertainties, an RBFNN is used. To our best knowledge, most motion-control problems have been solved by means of velocity or force controllers (Hong, Tamba, and Song 2008; Bugeja et al. 2009; Fallaha et al. 2011; Cheng et al. 2012). A drawback in this approach becomes particularly evident when the voltage-to-force (or voltage-to-velocity) transformation has nonlinearities. Therefore, instructions from the computer in the form of voltage input might be inaccurately transmitted to force or velocity. Recent studies on the assurance of safety have noted that modelling errors and uncertainties are important problems to be solved.

Our contributions are as follows. First, we design, for the driving and steering motors of a rear-steered wheeled vehicle, a voltage-input control law that can reduce the effects of modelling errors and additional uncertainties specifically by utilising a combination of a PD-type/sliding-mode voltage-input control law with RBFNN-based compensators. Secondly, we improve the safety of vehicles by consideration of collision cones. The designed sliding surface in the steering-control law is adjusted to meet the collision-cone-based safety criteria for solving the collision-avoidance problem. Also, the boundary of the driving velocity that keeps the vehicle in a safe configuration is introduced.

This paper is organised as follows. Section 2 describes the problem of the design of motion-control laws and estimators for modelling errors and uncertainties. Section 3 discusses the proposed controller's driving velocity and steering-angle designs. Section 4 conducts a safety analysis of the vehicle and investigates the relationship between safety and the design of the sliding-mode-based steering-control law. Section 5 presents simulation results of the performance of the proposed control law. Finally, Section 6 draws conclusions and discusses future research directions.

2. Problem description

In Figure 1, let O_b be the point of interest of a wheeled vehicle, (x, y) and θ represent the position of O_b in the global Cartesian space and its orientation with respect to

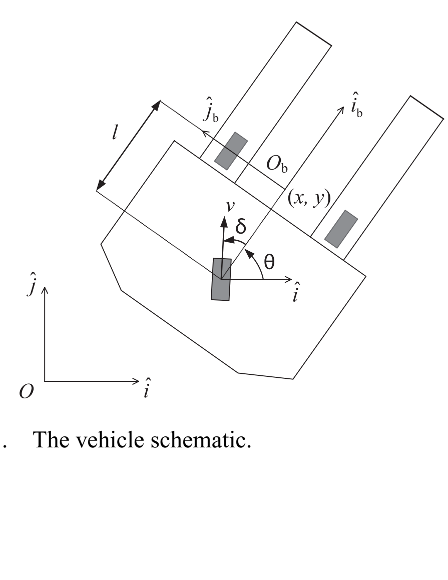

Figure 1. The vehicle schematic.

the global $\hat{i}$-axis, respectively, v and δ be the driving velocity and the steering angle of the vehicle, respectively, and l be the distance between the center of the rear wheelbase and O_b. Henceforth, the term 'configuration' is used to represent (x, y) and θ. The kinematics model of the vehicle in Figure 1 is provided as follows (Laumond, Jacobs, Taix, and Murray 1994; Li and Chang 2003; Tamba, Hong, and Hong 2009; Widyotriatmo and Hong 2012):

$$\dot{x} = v \cos\theta \cos\delta, \tag{1}$$

$$\dot{y} = v \sin\theta \cos\delta, \tag{2}$$

$$\dot{\theta} = -(v/l) \sin\delta. \tag{3}$$

The orientation θ is assumed to have a value in the interval of $-\pi \le \theta \le \pi$, and the admissible steering angle δ is in the interval $-\pi \le \delta \le \pi$.

Let m be the vehicle's mass, and I_b and I_δ be the moments of inertia of the vehicle with respect to O_b and that of the rear wheel with respect to the normal axis to the ground surface, respectively. Further, let I_r and I_f be the mass moments of inertia of the rear and front wheels, respectively; r_r and r_f be the radii of the rear and front wheels, respectively; φ_r and φ_f be the rear and front rotation angles of the rear and front wheels, respectively, and $\boldsymbol{p} = [x\ y\ \boldsymbol{\theta}\ \boldsymbol{\delta}\ \boldsymbol{\varphi}_f\ \boldsymbol{\varphi}_r]^T \in \Re^6$ the state vector of the vehicle. We adopt the following dynamic model for two-wheeled mobile robots (Widyotriatmo and Hong 2011):

$$\boldsymbol{M}(\boldsymbol{p})\ddot{\boldsymbol{p}} + \boldsymbol{C}(\boldsymbol{p}, \dot{\boldsymbol{p}})\dot{\boldsymbol{p}} + \boldsymbol{f} + \boldsymbol{g}(p) = \boldsymbol{B}\tau - \boldsymbol{J}(p)\boldsymbol{f}_c, \tag{4}$$

where $\boldsymbol{M}(\boldsymbol{p}) = \mathrm{diag}\{m, m, I_b, I_\delta, I_f, I_r\}$ is the inertia matrix, $C(p, \dot{p}) \in \Re^{6\times 6}$ is the centripetal and Coriolis matrix, $\boldsymbol{f} \in \Re^6$ is the vector of frictional forces, $\boldsymbol{g}(\boldsymbol{p}) \in \Re^6$ is the gravitational vector, $\boldsymbol{B}(\boldsymbol{p}) \in \Re^{6\times 2}$ is the input transformation matrix, $\boldsymbol{\tau} \in \Re^6$ is the vector of torque, $\boldsymbol{f}_c \in \Re^4$ is the vector of constraint forces and $\boldsymbol{J}(\boldsymbol{p})$ is the constraint matrix, given as (Widyotriatmo and Hong 2012)

$$\boldsymbol{J}(\boldsymbol{p}) = \begin{bmatrix} -\sin\theta & -\sin(\theta+\delta) & \cos\theta & \cos(\theta+\delta) \\ \cos\theta & \cos(\theta+\delta) & \sin\theta & \sin(\theta+\delta) \\ 0 & -l\cos\delta & 0 & -l\sin\delta \\ 0 & 0 & 0 & 0 \\ 0 & 0 & -r_f & 0 \\ 0 & 0 & 0 & -r_r \end{bmatrix}. \tag{5}$$

Let $\boldsymbol{v} = [\,v\ \dot{\delta}\,]^T$. Let the kernel of $\boldsymbol{J}(\boldsymbol{p})$ [i.e. $\boldsymbol{S}^T(\boldsymbol{p})\boldsymbol{J}(\boldsymbol{p}) = 0$] be

$$\boldsymbol{S}(\boldsymbol{p}) = \begin{bmatrix} \cos\theta\cos\delta & \sin\theta\cos\delta & -(1/l)\sin\delta & 0 & (1/r_f)\cos\delta & (1/r_r) \\ 0 & 0 & 0 & 1 & 0 & 0 \end{bmatrix}^T. \tag{6}$$

Then, the first and second time derivatives of $\boldsymbol{p}$ are given as

$$\dot{\boldsymbol{p}} = \boldsymbol{S}(\boldsymbol{p})\boldsymbol{v}, \tag{7}$$

$$\ddot{\boldsymbol{p}} = \dot{\boldsymbol{S}}(\boldsymbol{p})\boldsymbol{v} + \boldsymbol{S}(\boldsymbol{p})\dot{\boldsymbol{v}}. \tag{8}$$

Replacing the terms $\dot{\boldsymbol{p}}$ and $\ddot{\boldsymbol{p}}$ in Equation (4) with Equations (7) and (8) and pre-multiplying Equation (4) by $\boldsymbol{S}^T(\boldsymbol{p})$ yields

$$m_1\dot{v} + c_1 v + r_r f_v = \tau_v, \tag{9}$$

$$I_\delta\ddot{\delta} + f_\delta = \tau_\delta, \tag{10}$$

where f_v and f_δ are the surface frictions along the linear and rotational motions of the rear wheel, respectively. The parameters in Equation (9) are defined as

$$m_1(\delta) = r_r((m + (I_f + (r_f)^2))\cos^2\delta + (I_b/l^2)\sin^2\delta + I_r), \tag{11}$$

$$c_1(\delta, \dot{\delta}) = r_r((I_b/l^2) - (I_f/(r_f)^2) - m)\cos\delta\sin\delta\dot{\delta}, \tag{12}$$

and τ_v and τ_δ represent the torques applied to the driving motor and the steering motor, respectively. As in Widyotriatmo and Hong (2012), the torques τ_v and τ_δ are designed as

$$\tau_v = (k_{m,v}/R_{m,v})[u_v - (k_{emf,v}/r_r)v], \tag{13}$$

$$\tau_\delta = (k_{m,\delta}/R_{m,\delta})(u_\delta - k_{emf,\delta}\dot{\boldsymbol{\delta}}), \tag{14}$$

where u_v and u_δ are the input voltages applied to the driving and steering motors, respectively, $k_{m,v}$, $R_{m,v}$ and $k_{emf,v}$ are the driving motor's torque constant, resistance and electromotive-and-gear-ratio-related constant, respectively, and $k_{m,\delta}$, $R_{m,\delta}$ and $k_{emf,\delta}$ are those of the steering motor, respectively. Let us define the following parameters from the vehicle, which are known:

$$a_{v,0} = m_1(\delta)R_{m,v}/k_{m,v}, \tag{15}$$

$$b_{v,0} = c_1 R_{m,v}/k_{m,v} + k_{emf,v}/r_r, \tag{16}$$

$$b_{\delta,0} = k_{emf,\delta}. \tag{17}$$

The values of the parameters in Equations (15)–(17) typically come from the vehicle's datasheet. However, because uncertainties exist, difficulties are encountered when attempting to determine their actual values at a given time instance. Therefore, general expressions of those uncertainty-accommodating parameters are introduced. Let a_v and b_v be the driving-motor-related parameters formulated as

$$a_v = a_{v,0} + \Delta a_v, \tag{18}$$

$$b_v = b_{v,0} + \Delta b_v, \tag{19}$$

and let a_δ and b_δ be those related to the steering motor, given by

$$a_\delta = a_{\delta,0} + \Delta a_\delta, \tag{20}$$

$$b_\delta = b_{\delta,0} + \Delta b_\delta, \tag{21}$$

where Δa_v and Δb_v are the modelling errors related to the driving motor, and Δa_δ and Δb_δ are those related to the steering motor, respectively. Therefore, Equations (9)–(14) can be rewritten as

$$a_{v,0}\dot{v} + b_{v,0}v = u_v + d_v, \tag{22}$$

$$a_{\delta,0}\ddot{\delta} + b_{\delta,0}\dot{\delta} = u_\delta + d_\delta, \tag{23}$$

where

$$d_v = -\Delta a_v \dot{v} - \Delta b_v v - R_{\mathrm{m},v} r_{\mathrm{r}} f_v / k_{\mathrm{m},v}, \tag{24}$$

$$d_\delta = -\Delta a_\delta \ddot{\delta} - \Delta b_\delta \dot{\delta} - R_{\mathrm{m},\delta} f_\delta / k_{\mathrm{m},\delta}. \tag{25}$$

Here, d_v and d_δ contain modelling errors, that is, $-\Delta a_v \dot{v} - \Delta b_v v$ and $-\Delta a_\delta \ddot{\delta} - \Delta b_\delta \dot{\delta}$, respectively, as well as the frictional uncertainties $-R_{\mathrm{m},v} r_{\mathrm{r}} f_v / k_{\mathrm{m},v}$ and $-R_{\mathrm{m},\delta} r_{\mathrm{r}} f_\delta / k_{\mathrm{m},\delta}$, respectively. It is assumed that d_v and d_δ are bounded.

The problem is described as follows. Given the equations of motion in Equations (22) and (23), design a voltage-input control law (u_v, u_δ) such that the driving and steering motors can be driven to track the desired driving velocity and steering angle, respectively. To design controllers that compensate for the uncertainties d_v and d_δ, these uncertainties must be estimated. Another problem to solve is the use of the designed steering control to accommodate the vehicle's collision-avoidance behaviour. It is interesting to approach this problem not by switching the desired actuator values, but by increasing the value of the sliding surface.

3. Control design

3.1 Control law for driving

For the driving motor, we define the control design problem as follows. Find u_v such that v approaches v_{d} as time approaches infinity. Since there are dynamic-model uncertainties revealed in Equations (22) and (23), the controller u_v is decomposed into the main term $u_{v,0}$ and the compensator component $u_{v,\mathrm{c}}$ as follows:

$$u_v = u_{v,0} + u_{v,c}. \tag{26}$$

Suppose that $u_{v,0}$ is modelled in a PD fashion as

$$u_{v,0} = a_{v,0}(\dot{v}_{\mathrm{d}} - k_{\mathrm{P},v}(v - v_{\mathrm{d}})) + b_{v,0}v, \tag{27}$$

where v_{d} is the desired driving velocity and $k_{\mathrm{P},v} > 0$ is the speed feedback coefficient. Substituting Equations (26) and (27) into Equation (9) yields

$$(\dot{v} - \dot{v}_{\mathrm{d}}) + k_{\mathrm{P},v}(v - v_{\mathrm{d}}) = u'_{v,\mathrm{c}} + d'_v, \tag{28}$$

where $u'_{v,\mathrm{c}} = u_{v,\mathrm{c}}/a_{v,0}$ and $d'_{v,\mathrm{c}} = d_{v,\mathrm{c}}/a_{v,0}$. Let $\varepsilon'_{v,\mathrm{c}} = v - v_{\mathrm{d}}$. Then, Equation (28) can be rewritten as

$$\dot{\varepsilon}_v + k_{\mathrm{D},v}\varepsilon_v = u'_{v,\mathrm{c}} + d'_v. \tag{29}$$

The uncertainty d'_v can be expressed as

$$d'_v = \hat{d}'_v + \varsigma_v, \tag{30}$$

where $\hat{d}'_v$ is the approximated uncertainty of d'_v and ζ_v is the approximation error related to d'_v. The approximation error ζ_v is considerable if the assumption of the number of uncertainty patterns performing $\hat{d}'_v$ is substantially distinct from the actual d'_v. In this work, we assume that the number of uncertainty patterns is 1.

The control design problem now becomes more specific: Design the compensator $d'_{v,\mathrm{c}}$ in Equation (29), given the uncertainty d'_v such that $\dot{\varepsilon}_v \to 0$ and $\varepsilon_v \to 0$ as time approaches infinity. To this end, we propose a method to estimate d'_v using a radial basis function neural network (RBFNN). The purpose of which is to approximate modelling errors and uncertainties. The RBFNN uses the linear velocity error ε_v in the input layer. As in the hidden layer, the following Gaussian function is used:

$$\sigma_v = \exp\left(-\frac{(\varepsilon_v - c_v)^2}{\lambda_v^2}\right), \tag{31}$$

where c_v is the center of the RBF hidden layer, which can be chosen arbitrarily under the assumption that c_v is the mean of the single uncertainty pattern of d'_v, and $\lambda_v > 0$ is the variance of the RBF hidden layer. Practically, the number

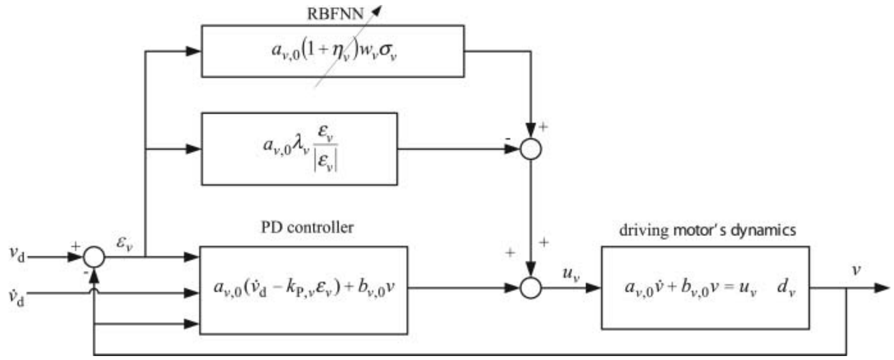

Figure 2. Control scheme of the driving motor.

of hidden layers in the RBFNN is the same as the number of assumed uncertainty patterns of d'_v. Since the number of uncertainty patterns is assumed to be 1 in this paper, the RBFNN consists of one hidden layer. The output layer of the RBFNN is d'_v, which is modelled, as a function of σ_v, as

$$\hat{d}'_v = w_v\sigma_v, \tag{32}$$

where w_v is the adjustable weight of the output layer. Let $n_v > 0$ be a learning coefficient that can be chosen without any restraint. The updating law of w_v is then given as

$$\dot{w}_v = -\eta_v\varepsilon_v\sigma_v. \tag{33}$$

A schematic of the driving motor control scheme is presented in Figure 2.

Proposition 1: *The RBFNN algorithm in Equations (31)–(33) is a universal estimator for d'_v.*

Proof: This proposition can be verified through the Stone–Weierstrass theorem of Cotter (1990). An exponential function is a compact function satisfying three necessary conditions for being a universal function: having the identity condition, separability property, and algebraic closure property. The RBFNN-based estimator in Equation (31) uses exponential functions that satisfy the properties of a universal estimator for d'_v, which is bounded. See Cotter (1990) for details. □

Remark 1: According to Cotter (1990), Proposition 1 leads to the guarantee of convergence of the RBFNN-based estimator in Equations (31)–(33).

Theorem 1: *Consider the driving motor with indefinite parameters as in Equation* (28) *and unknown disturbance d_v approximated by a neural network as in Equations* (31) *and* (32). *The driving velocity v will follow the desired driving velocity v_d, which implies that the velocity error $\varepsilon_v = v - v_d$ converges to zero if the controller and the learning algorithm of the neural network are chosen as*

$$u_v = a_{v,0}(\dot{v}_d - k_{P,v}\varepsilon_v) + b_{v,0}v + b_{v,0}\hat{u}'_v, \tag{34}$$

$$\hat{u}'_v = \left[(1+\eta_v)\,w_v\sigma_v - \lambda_v\frac{\varepsilon_v}{|\varepsilon_v|}\right], \tag{35}$$

where $k_{P,v}$, η_v, $\lambda_v > 0$.

Proof: Introduce the Lyapunov candidate function candidate as

$$V_v = 1/2[(\varepsilon_v)^2 + (w_v)^2]. \tag{36}$$

It can be determined that $V_v > 0$ when ε_v, $w_v \neq 0$; $V_v = 0$ if and only if ε_v, $w_v = 0$; and $V_v \to 0$ when ε_v, $w_v \to 0$. The time derivative of V_v is

$$\dot{V}_v = \varepsilon_v\dot{\varepsilon}_v + w_v\dot{w}_v. \tag{37}$$

From Equation (29), the following is derived:

$$\dot{\varepsilon}_v = \hat{u}'_{v,c} - d'_v - k_{P,v}\varepsilon_v. \tag{38}$$

Substituting Equation (33) into Equation (37) yields

$$\dot{V}_v = \varepsilon_v\left(\hat{u}'_{v,c} - d'_v - k_{P,v}\varepsilon_v\right) - w_v\dot{w}_v. \tag{39}$$

Then, substituting Equations (32) and (35) into Equation (39), we have

$$\dot{V}_v = -k_{P,v}\varepsilon_v^2 + \left(\hat{u}'_{v,c} - (1+\eta_v)\,w_v\sigma_v - \varsigma_v\right)\varepsilon_v. \tag{40}$$

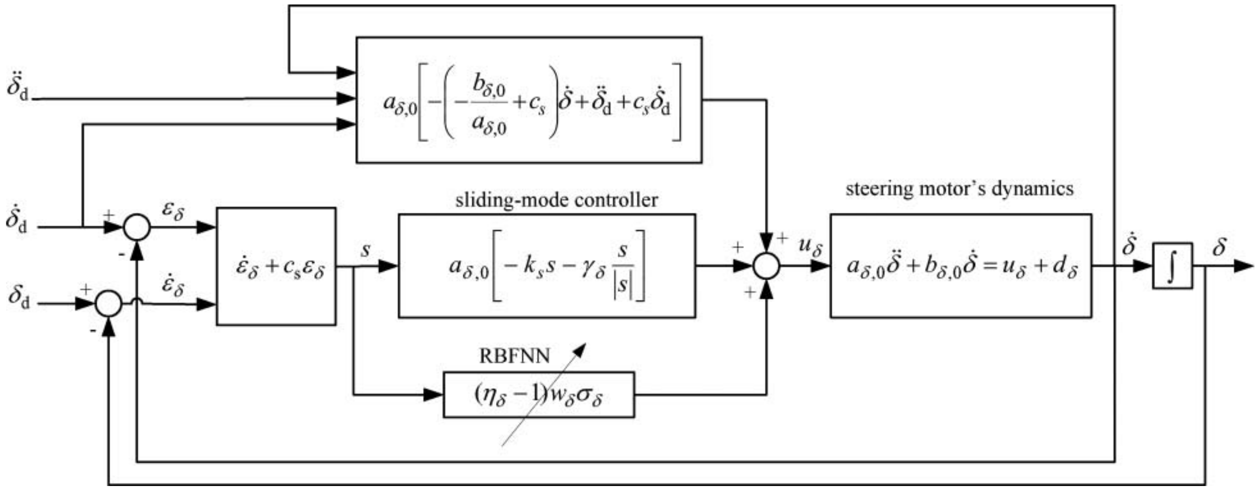

Figure 3. Control scheme of the steering motor.

Substituting Equation (35) into Equation (40) yields

$$\begin{aligned}\dot{V}_v &= -k_{\mathrm{P},v}\epsilon_v^2 - \lambda_v \frac{\epsilon_v^2}{|\epsilon_v|} - \sigma_v \epsilon_v \\ &\le -k_{\mathrm{P},v}\epsilon_v^2 - \lambda_v |\epsilon_v| - |\sigma_v||\epsilon_v| \\ &\le -k_{\mathrm{P},v}\epsilon_v^2 - \lambda_v |\epsilon_v| - |\epsilon_v| \sigma_{v,0}\,. \end{aligned} \tag{41}$$

Choose $\lambda_v = -\zeta_{v,0} + \mu_v$, $\mu_v > 0$. Then, Equation (41) can be rewritten as

$$\dot{V}_v = -k_{\mathrm{P},v}\varepsilon_v^2 - \lambda_v \frac{\varepsilon_v^2}{|\varepsilon_v|} - \varsigma_v \varepsilon_v \le -k_{\mathrm{D},v}\varepsilon_v^2 - \mu_v |\varepsilon_v| \le 0. \tag{42}$$

The time derivative of the Lyapunov candidate function $\dot{V}_v < 0$ when $\varepsilon_v \neq 0$ and $\dot{V}_v = 0$ only if $\varepsilon_v = 0$. Therefore, Equation (9) is globally asymptotically stable, and $v \to v_\mathrm{d}$ implies that the motor speed closely follows the desired velocity with the velocity error approaching 0. Theorem 1 is proved. □

3.2 *Control law for steering*

For the steering system, we define the control design problem as follows. Find u_δ such that δ approaches δ_d as time goes to infinity. Since typically the steering-control law is expressed as the steering angle without any specification of its desired change rate, we model the steering-control law differently from the driving velocity control law. For the steering system control design, we utilise a sliding surface $s(t)$ defined as

$$s = \dot{\varepsilon}_\delta + c_s \varepsilon_\delta, \tag{43}$$

where c_s is a positive constant and $\varepsilon_\delta = \delta - \delta_\mathrm{d}$. Therefore, Equation (10) can be rewritten as

$$a_{\delta,0}\ddot{\delta} + b_{\delta,0}\dot{\delta} = u_\delta + d_\delta(s). \tag{44}$$

The unknown $d_\delta(s)$ is the main rationale for reducing the control quality. Let $u'_\delta = u_\delta / a_{\delta,0}$ and $d'_\delta = d_\delta / a_{\delta,0}$. Then, Equation (44) can be rewritten as

$$\ddot{\delta} + \frac{b_{\delta,0}}{a_{\delta,0}}\dot{\delta} = u'_\delta + d'_\delta(s). \tag{45}$$

We model the uncertainty d'_δ as

$$d'_\delta = \hat{d}'_\delta + \varsigma_\delta, \tag{46}$$

where $\hat{d}'_\delta$ and ζ_δ are the approximation of d'_δ and the approximation error of d'_δ, respectively. Similarly to the driving motor case, for the approximation of the function $\hat{d}_\delta$, the disturbance model is chosen as follows:

$$\hat{d}'_\delta = w_\delta \sigma_\delta, \tag{47}$$

where w_δ is the weight of the output layer and

$$\sigma_\delta = \exp\left(-\frac{(\varepsilon_\delta - c_\delta)^2}{\lambda_\delta^2}\right). \tag{48}$$

The visualisation of the steering motor control scheme is presented in Figure 3. The control problem is now to find control u'_δ and a learning algorithm for $\dot{w}_\delta$ of the neural network in Equation (48) so that $s \to 0$ and the system slides toward the origin $\varepsilon_\delta = 0$ as $\delta \to \delta_\mathrm{d}$.

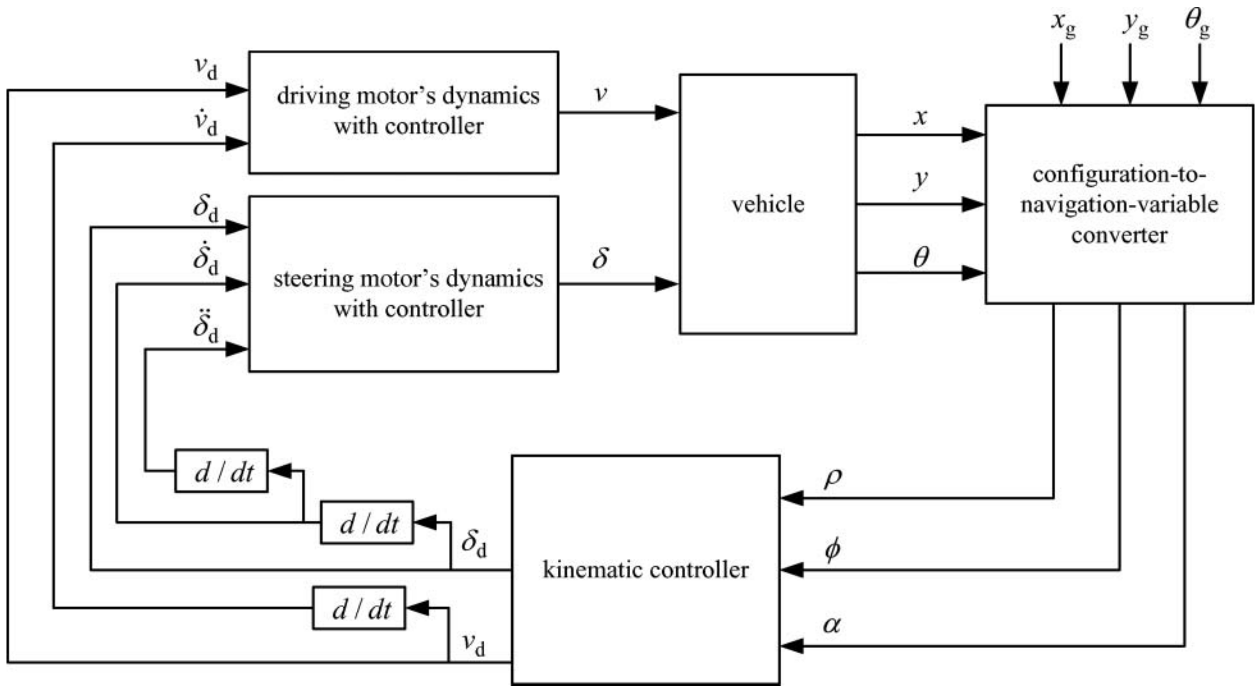

Figure 4. Motion control scheme of the vehicle.

Proposition 2: *The RBFNN algorithm in Equations* (47) *and* (48) *is a universal estimator for* d'_δ.

Proof: This proposition is verified similarly to Proposition 1. □

Remark 2: According to Cotter (1990), Proposition 2 leads to the guarantee of convergence of the RBFNN-based estimator in Equations (47) and (48).

Theorem 2: *The dynamic steering system in Equation* (10) *with the neural network in Equation* (48) *and the sliding surface shown in Equation* (43) *will follow the desired steering angle* d_δ *as the error* $\varepsilon_d \to 0$ *if the following control and learning algorithms are applied:*

$$u_\delta(t) = a_{\delta,0}\left[-\left(-\frac{b_{\delta,0}}{a_{\delta,0}} + c_s\right)\dot{\delta} + \ddot{\delta}_d + c_s\dot{\delta}_d - k_s s - \gamma_\delta \frac{s}{|s|}\right] + (\eta_\delta - 1) w_\delta \sigma_\delta, \tag{49}$$

$$\mathrm{d}w_\delta/\mathrm{d}t = -\eta_\delta s \sigma_\delta / a_{\delta,0}, \tag{50}$$

where k_s, η_δ, and γ_δ are positive constants.

Proof: The following Lyapunov function candidate is considered:

$$V_\delta = 1/2s^2 + 1/2(w_\delta)^2. \tag{51}$$

According to Equation (51), $V_\delta = 0$ if and only if $s = 0$ and $w_\delta = 0$. The time derivative of V_δ is given as

$$\dot{V}_\delta = s\dot{s} + w_\delta \dot{w}_\delta = s\left(\ddot{\varepsilon}_\delta + c_s\dot{\varepsilon}_\delta\right) + w_\delta \dot{w}_\delta. \tag{52}$$

From Equation (45), Equation (52) can be rewritten as

$$\dot{V}_\delta = s\left[\left(c_s - \frac{b_{\delta,0}}{a_{\delta,0}}\right)\dot{\delta} + \frac{u_\delta}{a_{\delta,0}} + d'_\delta - \ddot{\delta}_d - c_s\dot{\delta}_d\right] + w_\delta \dot{w}_\delta. \tag{53}$$

Applying Equations (46) and (47) and (49)–(51) to Equation (53) yields

$$\begin{aligned}\dot{V}_\delta &= -k_s s^2 - \gamma_\delta |s| + (\eta_\delta w_\delta s \sigma_\delta + s\varsigma_\delta) - w_\delta \eta_\delta s \sigma_\delta \\ &= -k_s s^2 - \gamma_\delta |s| + s\varsigma_\delta.\end{aligned} \tag{54}$$

By choosing $\gamma_\delta = -\zeta_\delta s/|s|$, $\mu > \zeta_{\delta,0}$ and applying it to Equation (54), we obtain

$$\dot{V}_\delta = -k_s s^2. \tag{55}$$

Therefore, $\dot{V}_\delta < 0$ for all $s \neq 0$ and $\dot{V}_\delta = 0$ if and only if $s = 0$. According to the Lyapunov stability theorem, we have $s \to 0$; and from Equation (55), the system will slide toward the origin $\varepsilon_\delta = 0$. This implies that $\delta \to \delta_d$. □

4. Safety analysis

Safe motion generation of automated guided vehicles has emerged as an important issue in recent years. Significantly, when applied inputs are taken into consideration, the classical collision-free paradigm for analysis of safety is no longer relevant. The main problem, then, has become: how to drive a vehicle such that some prohibited ICSs can be avoided in a finite time. In the present study, therefore, we adopt the ICS as an alternative scheme for collision-free paradigm. For details on the ICS, readers should refer to the work of Fraichard and Asama (2004). For safety analysis purposes, meanwhile, we adopt the approach proposed by Chakravarthy and Ghose (2012) known as the 'collision cone' (see Figure 5). The vectors of the linear velocities of the vehicle and some obstacles determine the utility of the control law for guaranteeing that the vehicle diverges from an obstacle-collision course at a certain future time instance.

Suppose that there exists a dynamic circular obstacle of radius R that has its center point located at (x', y'). The magnitude of the obstacle's velocity is represented by v', and its direction by the inclination angle with respect to the global $\hat{i}$-axis, denoted as θ'. Let ρ' and β, respectively, be the distance of the vehicle to an obstacle and the inclination angle of the vehicle-to-obstacle vector with respect to the vehicle's local $\hat{i}_b$-axis, which are given as

$$\begin{bmatrix} \rho' \\ \beta \end{bmatrix} = \begin{bmatrix} \sqrt{(x'-x)^2 + (y'-y)^2} \\ \arctan 2(y'-y, x'-x) - \theta \end{bmatrix}. \tag{56}$$

Also, let φ' represent the inclination angle of the obstacle's orientation with respect to the vehicle-to-obstacle vector.

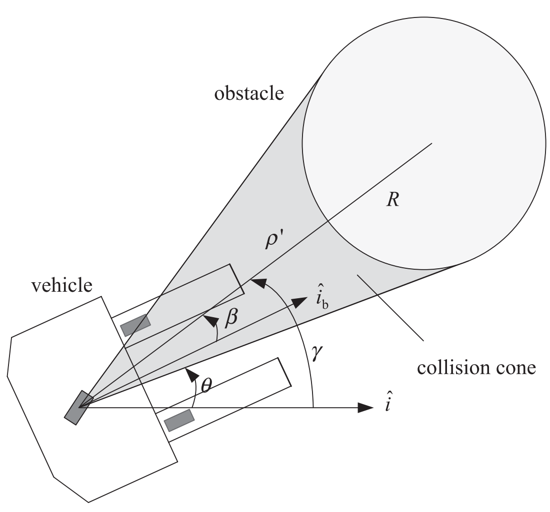

Figure 5. Collision cone.

The navigation variables are now expressed as

$$\begin{bmatrix} \dot{\rho}' \\ \dot{\beta} \end{bmatrix} = \begin{bmatrix} -\cos\beta\cos\delta & 0 & \cos\boldsymbol{\varphi}' \\ -\sin\beta\sin\delta/\boldsymbol{\rho}' & -1 & \sin\boldsymbol{\varphi}'/\boldsymbol{\rho}' \end{bmatrix} \begin{bmatrix} v \\ \omega \\ v' \end{bmatrix}, \tag{57}$$

where v and ω represent the actual driving velocity and the changing rate of the inclination angle of the vehicle-to-obstacle vector with respect to the vehicle's local $\hat{i}_b$-axis, respectively. Let γ be the inclination angle of the vehicle-to-obstacle vector with respect to the global $\hat{i}$-axis, $v_\gamma = \rho\prime\dot{\gamma}$ and $v_{\rho\prime} = \dot{\rho}\prime$. According to the collision-cone approach, a vehicle is said to be on a collision course with an obstacle if and only if there exists a ray from the vehicle to a point in the boundary of the obstacle such that $v_\gamma = 0$ and $v_{\rho'} < 0$. This definition is a 2-D version of Lemma 3 in Chakravarthy and Goshe (2012). Under constant linear velocities of the vehicle and obstacle, the necessary and sufficient conditions of $\rho^2(v_\gamma)^2 \leq R^2((v_\gamma)^2 + (v_{\rho'})^2)$ and $\dot{\rho}' < 0$ lead the vehicle and the obstacle to collide with each other at a certain future time instance (see Lemma 4, Chakravarthy and Goshe 2012). Therefore, additional conditions that violate the collision occurrence conditions are needed. To that end, we introduce the following function:

$$q = (R')^2((v_\gamma)^2 + (v_\gamma)^2) - (\rho')^2(v_\gamma)^2, \tag{58}$$

where $R' = R + \varepsilon_R$, ε_R being a small positive constant. Note that according to Chakravarthy and Goshe (2012), $q \geq 0$ implies that the vehicle is on a collision course with the obstacle, under the assumption that the linear velocities of the vehicle and obstacle are constants. Therefore, our concern here is the situation in which there is a collision-course configuration. Hence, to drive the vehicle out of the collision course, q should be driven to zero. Accordingly, the following function is defined:

$$V_s = 1/2\ q^2. \tag{59}$$

The time derivative of V_s is described as

$$\begin{aligned} \dot{V}_s = & -2v_{\rho'}\rho'\left(R^2 - \rho'^2\right)v_\gamma^4 + 2\dot{v}_\gamma\left(R^2 - \rho'^2\right)^2 v_\gamma^3 \\ & + 2v_{\rho'}R^2\left(\dot{v}_{\rho'}\left(R^2 - \rho'^2\right) - \rho' v_{\rho'}^2\right)v_\gamma^2 \\ & + 2\dot{v}_\gamma v_{\rho'}^2 R^2\left(R^2 - \rho'^2\right)v_\gamma + 2\dot{v}_{\rho'}R^4 v_{\rho'}^3. \end{aligned} \tag{60}$$

Note that since the investigation is focused on the collision-course exit problem, we set $\dot{\rho}' < 0$. We investigate the sufficient condition of $\dot{v}_{\rho'}$ by making the term $2\dot{v}_{\rho'}R^4 v_{\rho'}^3$ in Equation (60) negative. Since $v_{\rho'} < 0$, we obtain the sufficient condition as

$$\dot{v}_{\rho'} > 0. \tag{61}$$

The sufficient condition of v_γ can be investigated by analysing the first and third terms of Equation (60) such that it yields a negative value for $\dot{V}$ as follows. The first part is designed such that the inequality

$$-2v_{\rho'}\rho'\left(R^2-\rho'^2\right)v_\gamma^4+2v_{\rho'}R^2 \times\left(\dot{v}_{\rho'}\left(R^2-\rho'^2\right)-\rho v_{\rho'}^2\right)v_\gamma^2<0 \tag{62}$$

is satisfied. From Equation (62), we obtain the expression

$$\dot{v}_{\rho'} < \rho' v_\gamma^2 / R^2 - \rho' v_\rho^2 / \left(\rho'^2 - R^2\right). \tag{63}$$

According to Equation (61), the term $\rho'(v_\gamma)^2/R^2$–$\rho'(v_\rho)^2/((\rho')^2$–$R^2)$ in Equation (63) must be positive. Therefore, a sufficient condition of v_γ is

$$(v_\gamma)^2 > (v_\rho)^2\, R^2/((\rho')^2 - R^2). \tag{64}$$

Now, assuming that the obstacle is static (i.e., $v' = 0$), the second time derivative of ρ' (i.e. $\dot{v}_{\rho'}$) can be derived as follows:

$$\dot{v}_{\rho'} = -\dot{v}\cos\beta\cos\delta + v\dot{\beta}\sin\beta\cos\delta + v\dot{\delta}\cos\beta\sin\delta \tag{65}$$

Under the boundedness assumption of dv/dt, v, $d\beta/dt$ and $d\delta/dt$, it can be concluded that the value of $dv_{\rho'}/dt$ in Equation (65) is bounded as well. Moreover, under the assumption of $\dot{\delta}_{\mathrm{d}} = 0$ and

$$(|\gamma_\delta| + |(\eta_\delta - 1)w_\delta\delta_\delta|/a_{\delta,0} + d_\delta/a_{\delta,0})|v| < \xi_\delta, \tag{66}$$

where $\xi_\delta > 0$ and finite, the sliding surface in Equation (43) to satisfy Equation (63) is designed as

$$\sup\ddot{\rho}' = \sup\dot{v} + \sup\left(v\dot{\beta}\right) + \sup\left(v\dot{\delta}\right) = \kappa\rho'\left(\frac{v_\gamma^2}{R^2} - \frac{\dot{\rho}'^2}{\left(\rho'^2 - R^2\right)}\right), \tag{67}$$

where $0 < \xi < 1$,

$$\sup\dot{v} = \left|\dot{v}_{\mathrm{d}} - k_{\mathrm{P},v}\varepsilon_v\right| + \frac{b_{v,0}}{a_{v,0}}\left|(2+\eta_v)\,w_v\sigma_v\right| - \lambda_v\frac{b_{v,0}}{a_{v,0}}\frac{\varepsilon_v}{|\varepsilon_v|}, \tag{68}$$

$$\sup\left(v\dot{\beta}\right) = \left|\left(\frac{1}{\rho'} - \frac{1}{l}\right)\right||v|^2 + \left|v'v\right|, \tag{69}$$

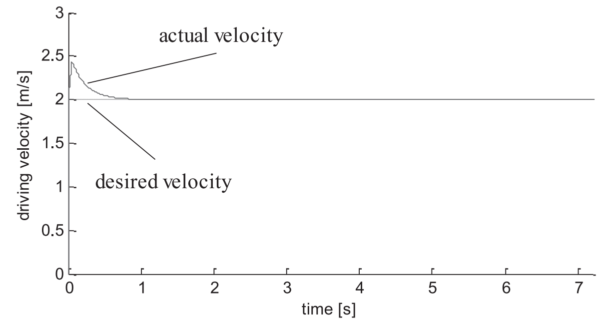

Figure 6. Driving velocity profile: desired velocity (dotted line, $v_{\mathrm{d}} = 2$ m/s) and actual velocity (solid line).

$$\sup\left(v\dot{\delta}\right) = \left|\dot{\delta}_{\mathrm{d}}v\right| + \frac{k_{\mathrm{s}}c_{\mathrm{s}}\,|\varepsilon_\delta v|}{(c_s + k_s)} + \frac{\xi_\delta}{(c_s + k_s)}\,|v|\,. \tag{70}$$

Now, the following auxiliary variables are introduced:

$$\xi_{s,1} = (0.5\kappa_{\rho'}(R^{-2}\,(v_\gamma)^2 - (\mathrm{d}\rho'/\mathrm{d}t)^2((\rho')^2 - R^2)^{-1})), \tag{71}$$

$$\xi_{s,2} = |((\rho')^{-1} - l^{-1})||v|^2 + |vv'|. \tag{72}$$

To determine the sufficient conditions of c_{s} and k_{s}, Equation (67) is rewritten as

$$\xi_{s,2} + (k_s c_s|\varepsilon_\delta v| + \xi_\delta)(c_s + k_s)^{-1} = \xi_{s,1}. \tag{73}$$

It is straightforward that the expression of k_{s} is

$$k_s = ((\xi_{s,1} - \xi_{s,2})c_s - \xi_\delta)(-(\xi_{s,1} - \xi_{s,2}) + c_s|\varepsilon_\delta v|). \tag{74}$$

Theorem 3: *If $(c_s)^2 > \xi_\delta\,|\varepsilon_\delta v|^{-1}$, the vehicle can move off from the collision course if the following sufficient conditions are satisfied:*

$$(1)\ v \le \xi_\delta|\varepsilon_\delta v|^{-1}\ \text{if}\ \xi_\delta(c_s)^{-1} < \xi_{s,1} - \xi_{s,2} < c_s|\varepsilon_\delta v|, \tag{75}$$

$$(2)\ v > \xi_\delta\,(c_s)^{-2}|\xi_\delta|^{-1},\ \text{elsewhere.} \tag{76}$$

Proof: According to Equation (55), $k_{\mathrm{s}} \ge 0$ makes steering system (44) asymptotically stable. There are two alternatives for achieving this goal. The first is to make both the numerator and denominator on the right-hand side of Equation (74) positive and the second is to make them negative. According to the first alternative, the range of $\xi_{s,1}$–$\xi_{s,2}$ to make $k_s \ge 0$ is $\xi_\delta/c_{\mathrm{s}} < (\xi_{\mathrm{s},1}$–$\xi_{\mathrm{s},2}) < c_{\mathrm{s}}|\xi_\delta\ v_{\mathrm{dr}}|$, on the basis of which it can be concluded that the driving velocity

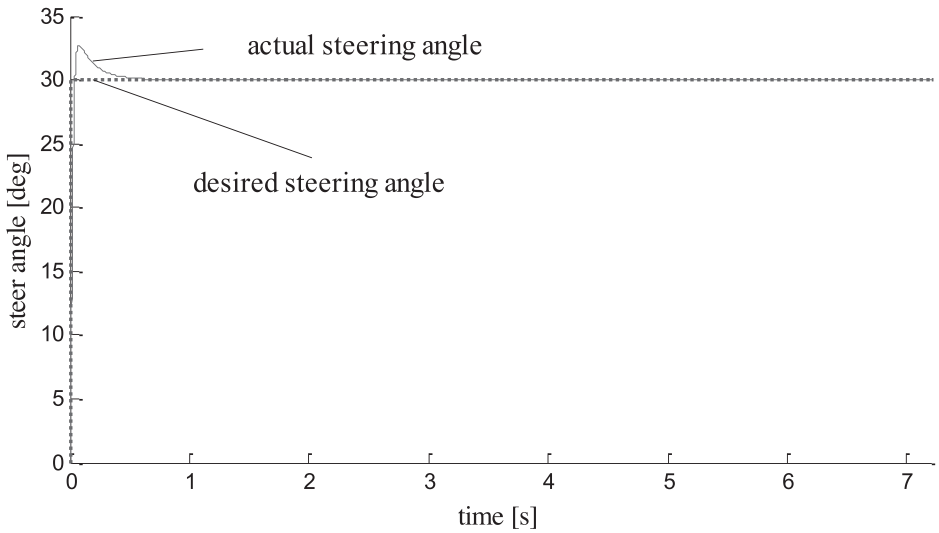

Figure 7. Steering angle profile: desired angle (dotted line, $\omega_d = 30°/s$) and actual angle (solid line).

should be $|v| > (\xi_{s,1}-\xi_{s,2}) > \xi_\delta\ (c_s)^{-1}$, and it is clear that by means of the second alternative, the range of $\xi_{s,1}-\xi_{s,2}$ is $(\xi_{s,1}-\xi_{s,2}) > c_s|\xi_\delta v_{dr}|$ or $(\xi_{s,1}-\xi_{s,2}) > \xi_\delta\ (c_s)^{-1}$. The theorem is proved. □

Theorem 4: *If $(c_s)^2 < \xi_\delta|\varepsilon_\delta v_{dr}|^{-1}$, the vehicle can move off from the collision course if the following sufficient conditions are satisfied:*

$$(1)\ v_{dr} \le \xi_\delta (c_s)^{-2}|\varepsilon_\delta|^{-1} \text{ if } \xi_{s,1}-\xi_{s,2} > \xi_\delta(c_s)^{-1} \text{ or } \xi_{s,1}-\xi_{s,2} < c_s|\xi_\delta v_{dr}|, \quad (77)$$

$$(2)\ v_{dr} > \xi_\delta (c_s)^{-2}|\varepsilon_\delta|^{-1}, \text{ elsewhere.} \quad (78)$$

Proof: The proof of this theorem is similar to that of Theorem 3. □

Theorem 5: *Assume that $\dot{v}_d = 0$ in Equation (27) with a constant proportional gain $k_{P,v}$. The following condition, then, is required for v_ρ to drive the vehicle off from the collision course:*

$$v_\rho < \sqrt{\left(\frac{v_\gamma^2}{R^2} - \frac{2}{\kappa\rho'}\left(\frac{b_{v,0}\,|(2+\eta_v)\,w_v\sigma_v|}{a_{v,0}} - |\varepsilon_v|\,|k_{P,v}|\right)\right)(\rho'^2 - R^2)}. \quad (79)$$

Proof: From Equations (67) and (68), it can be determined that

$$|\lambda_v| < \frac{a_{v,0}}{b_{v,0}\,|\varepsilon_v|}\left(\xi_{s,1} - \left|\dot{v}_{dr}^*\right|\right) - \frac{|(2+\eta_v)\,w_v\sigma_v|}{|\varepsilon_v|} - \frac{a_{v,0}}{b_{v,0}}\left|k_{P,v}\right|. \quad (80)$$

For the left-hand side of Equation (80) to exist, the right-hand side must be positive. Therefore, the theorem is proved. □

5. Simulation results

The overall motion-control scheme is depicted in Figure 4. Let ρ, α and φ denote the distance between the vehicle and the goal point, the inclination angle made by the local $\hat{i}_b$-axis of the vehicle and the vehicle-to-reference point, respectively. In summary, given the goal configuration (x_g,y_g,θ_g), the driving and steering motors have to apply driving velocity v and steering-angle δ such that the navigation variables ρ, α and φ approach infinity in a finite time. The kinematic controller processes those variables into the desired driving velocity v_d and steering angle ω_d.

In this section, the performance of the proposed control law is presented. Some of the parameter values are set as in Widyotriatmo and Hong (2012): the mass of the vehicle is $m = 1{,}500$ kg, and the moments of inertia are $I_b = 350$ kg m^2, $I_\delta = 350$ kg m^2, $I_f = 0.1$ kg m^2 and $I_r = 0.6$ kg m^2; the radii of the front and rear wheels are $r_f = 25$ mm and $r_r =$

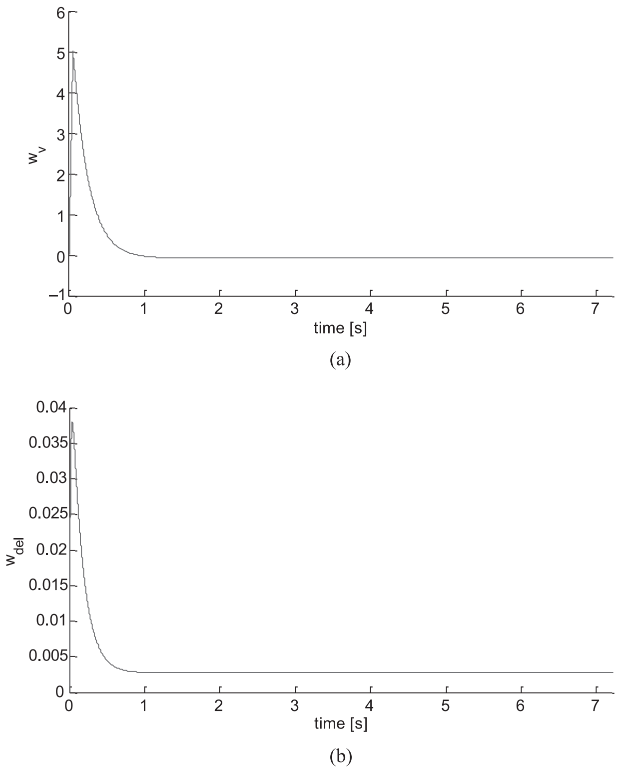

Figure 8. Output weight profiles.

150 mm, respectively; the motor parameters are $k_{m,v} = k_{m,\delta} = 87.7$ Nm/A, $R_{m,v} = R_{m,\delta} = 0.75\ \Omega$, $k_s = 10$ and $k_{D,v} = 10$ V s^2 m^{-1}, respectively, and the RBFNN parameters are $n_v = 1$, $\lambda_v = 10^3$, $\lambda_\delta = 10^5$, $c_v = 10^5$, $\eta_\delta = a_\delta/50$, $c_\delta = 10$ and $c_s = 2000$, respectively.

Figures 6 and 7 demonstrate the performance of the proposed control law and estimation method for given constants v_d and ω_d. The velocities were set to $v_d = 2$ m s^{-1} and $\delta_d = 30^o$, respectively The initial values of the output layers' weights were $w_v = 0$ and $w_\delta = 0$. As shown in Figure 6, the desired velocity is attained in 1.5 s. Moreover, as shown in Figure 7, the desired steering angle is achieved in no more than 1 s. It can be concluded, therefore, that the proposed control law works good in this situation. The profiles of weights w_v and w_δ of the RBFNN outputs are plotted in Figure 8, which shows that when the desired driving velocity and steering angle are tracked accurately, w_v goes to zero and w_δ tends to 0.0027 as time approached infinity.

Figures 9∼11 demonstrate the performance of the control law and estimation method for a point-stabilisation problem in a simple workspace involving a circular obstacle of radius $r_{obs} = 1$ m. Here, the desired driving velocity and steering angle are designed as follows:

$$v_d = \left((k_{v,1}\rho\cos\alpha)^2 + l^2(k_{v,2}\sin\alpha - (k_{v,2} - k_{v,1}\cos\alpha)\phi)^2\right)^{0.5}, \quad (81)$$

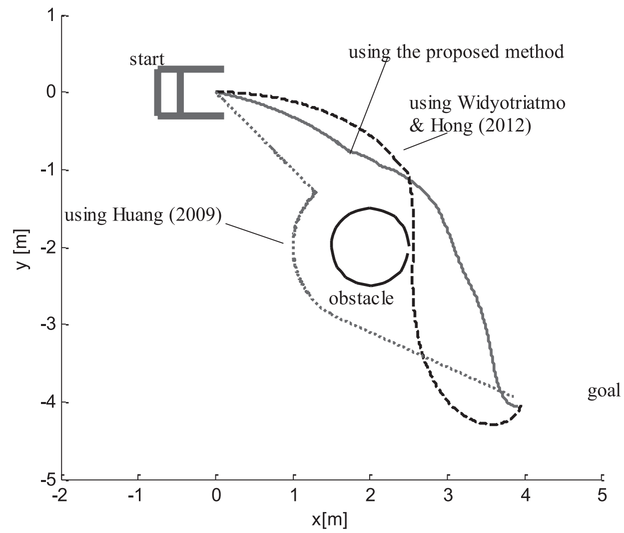

Figure 9. Comparison of the generated paths for point stabilisation.

$$\delta_d = -\arctan\left(l\ \left(\left(k_{v,2}\sin\alpha - (k_{v,2} - k_{v,1}\cos\alpha)\phi\right)/(k_{v,1}\rho\cos\alpha)\right)\right). \quad (82)$$

The coefficients in Equations (81) and (82) are set to $k_{v,1} = 0.5$ s^{-1} and $k_{v,2} = 5$ s^{-1}. In this scenario, the initial configuration of the vehicle is set to $(x, y, \theta) = (0$ m, 0 m, $0^o)$, and the goal configuration is given by $(x_g, y_g, \theta_g) = (4$ m, -4 m, $0^o)$. The obstacle occupies the point $(x'\ y') = (2$ m, 2 m). In our algorithm, we apply Theorems 3–5 when the conditions therein are satisfied, which means that the vehicle lies in a collision course with the obstacle.

Under this particular condition, the sliding surface's parameter is set to $c_s = -0.01$. Under the normal condition (i.e. the vehicle is not on a collision course), the parameter would be set at $c_s = -0.01$. The purpose of setting $c_s < 0$ is to make a large steering-angle deviation in the presence of the obstacle. The generated paths of the original algorithm of Widyotriatmo and Hong (2012) and the modified algorithm are shown in Figure 9. As the method of Widyotriatmo and Hong (2012) lacks any obstacle-avoidance feature, the vehicle might collide with the obstacle. With our proposed method and its obstacle-avoidance algorithm, the vehicle, despite approaching very close to the obstacle at a particular time, was able to avoid it, as illustrated in Figure 9.

A comparison to another work reported by Huang (2009) is provided in Figure 9 as well, where a potential field-based velocity planning was compared. This method utilises the concept of attractive and repulsive forces generated by the goal point and the center of the obstacle, respectively. The proposed controller was

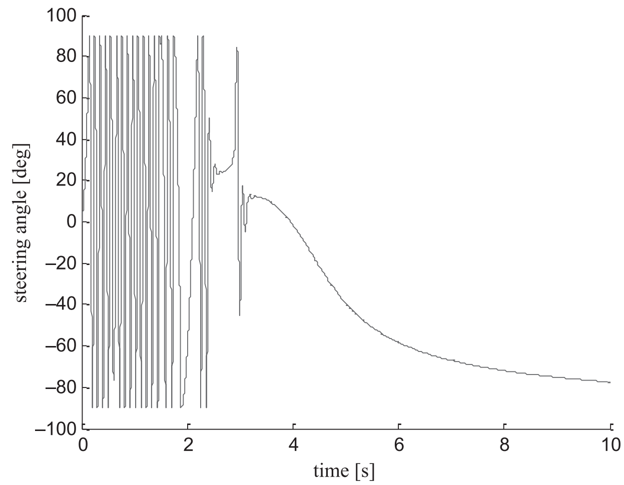

Figure 10. Steering angle of the vehicle.

defined as

$$v = \begin{cases} \kappa_{\mathrm{att}}\mathrm{P} - \kappa_{\mathrm{rep}} R^{-2} \|\mathrm{P}'\|^{-1} (R^{-1} - R_0^{-1})\mathrm{P}', & \text{if } \rho' \leq R_0, \\ \kappa_{\mathrm{att}}\mathrm{P}, & \text{elsewhere}, \end{cases} \tag{83}$$

where $\boldsymbol{v}$ is the velocity vector of the vehicle, $\boldsymbol{P}$ and $\boldsymbol{P'}$ are the vehicle-to-goal and vehicle-to-obstacle vectors, respectively, κ_{att} and κ_{rep} are the attractive and repulsive scaling factors, respectively, and R_0 is defined as the radius of the influence area of the obstacle. In this comparison, we set $\kappa_{\mathrm{att}} = 0.2$, $\kappa_{\mathrm{rep}} = 0.4$, $R_0 = 2$ m. However, the potential function based algorithm has a drawback: the length of the influence area's radius might cause failure in motion generation processes. A simple example is when the vehicle starts in the influence area: if the values of κ_{att} and κ_{rep} are not proper, the vehicle might fail to reach the goal point since the repulsive force is larger than the attractive one. The generated path in Figure 9 is an example of a successful motion generation.

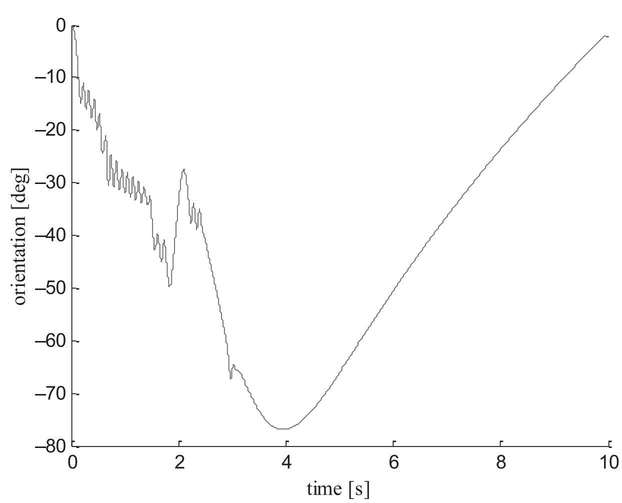

Figure 11. Orientation angle of the vehicle.

The collision-avoidance feature in our proposed method is actually potentiated by the change of the sliding-mode parameter from a positive value to a negative value, which increases the value of the sliding surface, and which in turn leads to an increased steering-angle error ε_δ. As shown in Figure 10, this approach drives the trajectory of the steering angle to its maximum and minimum values. Figure 11 reveals the vehicle's orientation, thereby demonstrating that the fluctuation of steering angle ε_δ leads to the fluctuation of vehicle orientation θ.

6. Conclusions

A sliding-mode control and RBFNN-based estimation method to compensate for modelling errors and additional uncertainties for a class of wheeled vehicles was proposed. A novel principle here was the achievement of obstacle avoidance by sliding-mode parameter adjustment. The proposed method has been incorporated into the existing navigation schemes to guarantee safe collision-free movement around obstacles. Simulation results revealed that the proposed method can track a planned driving velocity and steering angle and, in so doing, enables successful avoidance of collisions. Future work is to extend the proposed method in improving the safety of multiple vehicles in dynamic environments.

Acknowledgements

This research was supported by the National Research Foundation of Korea funded by the Ministry of Education, Science and Technology, Korea (No. MEST-2012-R1A2A2A01046411) and the World Class University Program (No. R31-20004).

Notes on contributors

Anugrah K. Pamosoaji received his BEng and MEng degrees in Electrical Engineering from the Bandung Institute of Technology, Indonesia, in 2003 and 2006, respectively. He is currently working toward his PhD in the School of Mechanical Engineering, Pusan National University, Korea. His research interests include robotics, path planning, control systems and multivehicle systems.

Pham Thuong Cat received his MS degree in Computer Engineering from the Budapest Technical University in 1972 and PhD in Control Engineering from the Hungarian Academy of Sciences (MTA) in 1977. From 1985 to 1988, he was a Postdoctoral Fellow at MTA SzTAKI, the Research Institute of Computer and Automation of MTA, and received his DSc degree in Robotics from the Hungarian Academy of Science in 1988. He is an Honorary Research Professor in Computational Sciences at MTA SzTAKI. Since 1979, he is involved in both research and teaching PhD courses at the Institute of Information Technology, Vietnamese Academy of Science and Technology. Dr Cat is also serving as the Editor-in-Chief of the *Journal of Computer Science and Cybernetics* of the Vietnamese Academy of Science and Technology. He is the Vice-President of the Vietnamese Association of Mechatronics. His research interests include robotics, control theory, cellular neural networks and embedded control systems. He co-authored four books and published over 140 papers on national and international journals and conference proceedings.

Keum-Shik Hong received his BSME from Seoul National University in 1979, his MSME from Columbia University, New York, in 1987, and both an MS degree in Applied Mathematics and a PhD in ME from the University of Illinois at Urbana in 1991. His laboratory was designated as a National Research Laboratory by the MEST of Korea in 2003. In 2009, under the World Class University Program, he established the Department of Cogno-Mechatronics Engineering. Dr Hong also served as the Editor-in-Chief of the *Journal of Mechanical Science and Technology* (2008–2011), AE of *Automatica* (2000–2006) and Deputy Editor-in-Chief of the *IJCAS* (2003–2005). He was also the General Secretary of the Asian Control Association (2006–2008), and the Organizing Chair of the ICROS-SICE International Conference 2009, Japan. He has received many awards including the Best Paper Award from the KFSTS of Korea (1999), the Harashima Mechatronics Award (2003), the Automatica Certificate of Outstanding Service (06), the Presidential Award of Korea (2007), the ICROS Achievement Award (2009), the IJCAS Contribution Award (2010), the Best Teaching Professor Award (2010), the IJCAS Award (2011) and the Premier Professor Award (2011), among others. Dr Hong's current research interests include brain–computer interface, adaptive control and distributed parameter systems.

References

Bugeja, M.K., Fabri, S.G., and Camilleri, L. (2009), 'Dual Adaptive Dynamic Control of Mobile Robots Using Neural Networks', *IEEE Transactions on Systems, Man, and Cybernetics-B*, 39, 129–141.

Chakravarthy, A., and Ghose, D. (2012), 'Generalization of the Collision Cone Approach for Motion Safety in 3-D Environments', *Autonomous Robot*, 32, 243–266.

Chang, Y.-H., Chang, C.-W., Chen, C.-L., and Tao, C.-W. (2012), 'Fuzzy Sliding-Mode Formation Control for Multi-robot Systems: Design and Implementation', *IEEE Transactions on Systems Man and Cybernetics-B*, 42, 444–457.

Chen, C.-H. (2011), 'Intelligent Transportation Control System Design Using Wavelet Neural Network and PID-Type Learning Algorithms', *Expert Systems with Applications*, 38, 6926–6939.

Cheng, M.-B., Su, W.-C., and Tsai, C.-C. (2012), 'Robust Tracking Control of a Unicycle-Type Wheeled Mobile Manipulator Using a Hybrid Sliding Mode Fuzzy Neural Network', *International Journal of Systems Science*, 43, 408–425.

Chwa, D. (2004), 'Sliding-Mode Tracking Control of Nonholonomic Wheeled Mobile Robots in Polar Coordinates', *IEEE Transactions on Control Systems Technology*, 12, 637–644.

Cotter, N.E. (1990), 'The Stone-Weierstrass Theorem and Its Applications to Neural Networks', *IEEE Transactions on Neural Networks*, 1, 290–295.

Deng J., Li K., and Irwin, G.W. (2012), 'Locally Regularised Two-Stage Learning Algorithm for RBF Network Centre Selection', *International Journal of Systems Science*, 43, 1157–1170.

Fallaha, C.J., Saad, M., Kanaan, H.Y., and Al-Haddad, K. (2011), 'Sliding-Mode Robot Control with Exponential Reaching Law', *IEEE Transactions on Industrial Electronics*, 58, 600–610.

Fierro, R., and Lewis, F.L. (1998), 'Control of a Nonholonomic Mobile Robots Using Neural Networks', *IEEE Transactions on Neural Networks*, 9, 589–600.

Fraichard, T., and Asama, H. (2004), 'Inevitable Collision States: a Step Towards Safer Robots?', *Advanced Robotics*, 18, 1001–1024.

Gan, Q., and Liang, Y. (2012), 'Synchronization of Non-identical Unknown Chaotic Delayed Neural Networks Based on Adaptive Sliding Mode Control', *Neural Processing Letters*, 35, 245–255.

Ge, S.S., and Zhang, J. (2003), 'Neural-Network Control of Non-affine Nonlinear System with Zero Dynamics by State and Output Feedback', *IEEE Transactions on Neural Networks*, 14, 900–918.

Hong, K.-S., Tamba, T.A., and Song, J.B. (2008), 'Mobile Robot Control Architecture for Reflexive Avoidance of Moving Obstacles,' *Advanced Robotics*, 22, 1397–1420.

Hornik, K. (1989), 'Multilayer Feedforward Networks are Universal Approximators', *Neural Networks*, 2, 359–366.

Hornik, K. (1991), 'Approximation Capabilities of Multilayer Feedforward Networks', *Neural Networks*, 4, 251–257.

Huang, L. (2009), 'Velocity Planning for a Mobile Robot to Track a Moving Target: a Potential Field Approach', *Robotics and Autonomous Systems*, 57, 55–63.

Kasac, J., Deur, J., Novakovic, B., Kolmanovsky, L.V., and Assadian, F. (2011), 'A Conjugate Gradient-Based BPPT-Like Optimal Control Algorithm with Vehicle Dynamics Control Application', *IEEE Transactions on Control Systems Technology*, 19, 1587–1595.

Khan, Q., Bhatti, A.I., Iqbal, M., and Ahmed, Q. (2012), 'Dynamic Integral Sliding-Mode Control for SISO Uncertain Nonlinear Systems', *International Journal of Innovative Computing, Information, and Control*, 8, 4621–4633.

Laumond, J.-P., Jacobs, P.E., Taix, M., and Murray, R.M. (1994), 'A Motion Planner for Nonholonomic Mobile Robots', *IEEE Transactions on Robotics and Automation*, 10, 577–593.

Li, T.H.S., and Chang, S.-J. (2003), 'Autonomous Fuzzy Parking Control', *IEEE Transactions on Systems, Man, and Cybernetics-A*, 33, 451–465.

Lin, T.-C., Chang, S.-W., and Hsu, C.-H. (2012), 'Robust Adaptive Fuzzy Sliding Mode Control for a Class of Uncertain Discrete-Time Nonlinear Systems', *International Journal of Innovative Computing, Information, and Control*, 8, 347–359.

Lin, Z., Xia, Y., Shi, P., and Wu, H. (2011),'Robust Sliding Mode Control For Uncertain Linear Discrete Systems Independent of Time-Delay', *International Journal of Innovative Computing, Information, and Control*, 7, 869–880.

Ngo, Q.H., and Hong, K.-S. (2012), 'Adaptive Sliding Mode Control of Container Cranes', *IET Control Theory and Applications*, 6, 662–668.

Ngo, Q.H., and Hong, K.-S. (2012), 'Sliding-Mode Anti-Sway Control of an Offshore Container Crane', *IEEE/ASME Transactions on Mechatronics*, 17, 201–209.

Park, B.S., Yoo, S.J., Park, B., and Choi, Y.H. (2009), 'Adaptive Neural Sliding Mode Control of Nonholonomic Wheeled Robots with Model Uncertainty', *IEEE Transactions on Control Systems Technology*, 17, 207–214.

Schilling, R.J., Carroll, J.J. , and Al-Ajlouni, A.F. (2001), 'Approximation of Nonlinear Systems with Radial Basis Function

Neural Network', *IEEE Transactions on Neural Networks*, 12, 1–15.

Shi, P., Xia, Y., Liu, G.P., and Rees, D. (2006), 'On Designing of Sliding-Mode Control for Stochastic Jump Systems', *IEEE Transactions on Automatic Control*, 51, 97–103.

Tamba, T.A., Hong, B., and Hong, K.-S. (2009), 'A Path Following Control of an Unmanned Autonomous Forklift', *International Journal of Control, Automation, and Systems*, 71, 113–122.

Tsai, C.-C., Chan, C.-K., and Li, Y.Y. (2012), 'Adaptive H_∞ Nonlinear Velocity Tracking Using RBFNN for Linear DC Brushless Motor', *International Journal of Systems Science*, 43, 63–72.

Widyotriatmo, A., and Hong, K.-S. (2011), 'Navigation Function-Based Control of Multiple Wheeled Vehicle', *IEEE Transactions on Industrial Electronics*, 58, 1896–1906.

Widyotriatmo, A., and Hong, K.-S. (2012), 'Switching Algorithm for Robust Configuration Control of a Wheeled Vehicle', *Control Engineering Practice*, 20, 315–325.

Widyotriatmo, A., Hong, B., and Hong, K.-S. (2009), 'Predictive Navigation of an Autonomous Vehicle with Nonholonomic and Minimum Turning Radius Constraints', *Journal of Mechanical Science and Technology*, 23, 381–388.

Widyotriatmo, A., Hong, K.-S., and Prayudhi, L.H. (2010), 'Robust Stabilization of a Wheeled Vehicle: Hybrid Feedback Control Design and Experimental Validation', *Journal of Mechanical Science and Technology*, 24, 513–520.

Wu, L., Shi, P., and Gao, H. (2010), 'State Estimation and Sliding-Mode Control of Markovian Jump Singular Systems', *IEEE Transactions on Automatic Control*, 55, 1213–1219.

Wu, L., Su, X., and Shi, P. (2012), 'Sliding Mode Control with Bounded L-2 Gain Performance of Markovian Jump Singular Time-Delay Systems', *Automatica*, 48, 1929–1933.

Xu, D., Zhao, D., Yi, J., and Tan, X. (2009), 'Trajectory Tracking Control of Omnidirectional Wheeled Mobile Manipulators: Robust Neural Network-Based Sliding Mode Approach', *IEEE Transactions on Systems, Man, and Cybernetics-B*, 39, 788–799.

Yang, S.X., Zhu, A., Yuan, G., and Meng, M.Q.-H. (2012), 'A Bioinspired Neurodynamics-Based Approach to Tracking Control of Mobile Robots', *IEEE Transactions on Industrial Electronics*, 59, 3211–3220.

Zhang, M.-J., and Chu, Z.-Z. (2012), 'Adaptive Sliding Mode Control Based on Local Recurrent Neural Networks for Underwater Robot', *Ocean Engineering*, 45, 56–62.

Zhang, T.-P., Zhu, Q., and Yang, Y.-Q. (2012), 'Adaptive Neural Control of Non-Affine Pure-Feedback Non-Linear Systems with Input Nonlinearity and Perturbed Uncertainties', *International Journal of Systems Science*, 43, 691–706.

Zhao, D, and Zhou, T. (2012), 'A Finite-Time Approach to Formation Control of Multiple Mobile Robots with Terminal Sliding Mode', *International Journal of Systems Science*, 43, 1998–2014.